ISSN 0029 - 3865

CPBF-NF-015/85

HELICITY AMPLITUDE ANALYSIS OF THE REACTION $\pi^+p \to \Delta^{++}(\pi^+\pi^-\pi^0)$ IN THE η^0 AND ω^0 REGION AT 16 GeV/c

by

A.M.F. Endler, P. Girtler* and H.V. Pinto**

Centro Brasileiro de Pesquisas Físicas - CBPF/CNPq
Rua Dr. Xavier Sigaud, 150
22290 - Rio de Janeiro, RJ - Brasil

*Institute für Theoretische Physik, Universität Innsbruck

**Universidade Federal Fluminense

ABSTRACT

An amplitude analysis has been performed for the reactions $\pi^+ p \to (\eta^0, \omega^0)\Delta^{++}$ at 16 GeV/c, constraining the relative spin between the target proton and the Δ^{++} to be 1. The amplitudes are determined in intervals of t' by a maximum likelihood fit. The quality of the fits is checked by comparing the experimental decay angular distributions of the η^0, ω^0 and Δ^{++} in the Gottfried-Jackson system. The structure observed in the magnitudes and phases of the obtained amplitudes is consistent with that expected on the basis of currently accepted phenomenological ideas.

Key-words: Amplitude analysis; High-energy interactions.

1. INTRODUCTION

In this paper we perform a helicity amplitude analysis of the reactions

$$\pi^+ p \to (\eta^0, \omega^0)\Delta^{++}$$

at 16 GeV/c from a sample of 34.225 events fitted for the reaction $\pi^+ p \to p\pi^+\pi^+\pi^-\pi^0$ (*) observed in the CERN 2m hydrogen bubble chamber. An amplitude analysis of the reaction $\pi^+ p \to \omega^0\Delta^{++}$ has been carried out at 7,1 GeV/c [1] and at 16 GeV/c [2].

The relative spin between the target proton and the Δ^{++} is constrained to be 1, according to the additivity assumption for the quark model as applied to high-energy scattering [3]. This constraint reduces the number of amplitudes necessary for describing the investigated reactions and was successfully applied in the amplitude analysis of the reaction $\pi^+ p \to (\pi^+\pi^-)\Delta^{++}$ in the ρ^0-region at 16 GeV/c [4] [5].

This paper is organized as follows. In section 2 the data sample and its purity are discussed. In section 3 we describe shortly the method (a detailed description is given in the appendix of the paper [4] and [5]). Section 4 contains, for the ω^0 and η^0 regions, the results of our analysis and the comparison between the experimental and the predicted angular distributions. In section 5 we give the conclusions and a comparison of our results for the reaction $\pi^+ p \to \omega^0\Delta^{++}$ with those obtained by the experiment at 7.1 GeV/c [1].

(*) We thank Prof. Otter and the members of the Aachen - Berlin - Bonn - CERN - - Cracow - Heidelberg Collaboration, who made us these data available.

2. THE DATA

The events used in this analysis are subsets consisting of 110 events (η^0 region) and 611 events (ω^0 region) from the above mentioned sample, which satisfy the following selection conditions:

$$\text{a)} \qquad 1.08 \leq M(p\pi_s^+) \leq 1,4 \tag{1}$$

$$\text{b)} \quad 0.52 \leq M(\pi_f^+\pi^-\pi^0) \leq 0.60 \quad (\eta^0 \text{ region})$$
$$0.72 \leq M(\pi_f^+\pi^-\pi^0) \leq 0.81 \quad (\omega^0 \text{ region})$$

where π_s^+ and π_f^+ mean the slowest π^+ and the fastest π^+, respectively.

In Fig. 1 we show the distribution of the effective mass $M(p\pi_s^+)$, where the presence of the Δ^{++} peak can be seen. The middle histogram corresponds to the data in which the $M(\pi_f^+\pi^-\pi^0)$ is in the ω^0 region and the upper histogram in the η^0 region.

In Fig. 2 we show the distribution of $M(\pi_f^+\pi^-\pi^0)$ with visible presence of the η^0, ω^0, A_2 peaks and a light indication of the ω^{0*}. The hatched histogram represents events with $M(p\pi_s^+)$ in the Δ^{++} (1236) region. The upper part of Fig. 2 shows the detailed region of the η^0 and ω^0 masses.

The background underneath the Δ^{++} (1236), η^0 (549) and ω^0 (783) resonances is small (about 5% for Δ^{++}, 10% for η^0 and 15% for ω^0) and can be considered negligible.

The selection procedure is tested analysing the other possibility of associating the mesons π^+. For this purpose we give in Fig. 3 the distribution of the $M(p\pi_f^+)$ where no evidence of Δ^{++} peak is seen.

To study the spin content which contributes to the reaction $\pi^+p \to (p\pi_s^+)(\pi_f^+\pi^-\pi^0)$ after the above mentioned cuts a) and b), we give in Fig. 4 for η^0 region and in Fig. 5 for ω^0 region, the normalized D-moments defined as

$$\langle D^J_{M0} \rangle = \frac{1}{N} \sum_{i=1}^{N} D^J_{M0}(\phi_i, \theta_i, 0) \quad ,$$

where ϕ, θ refer to the decay angle of the $\pi_f^+\pi^-\pi^0$ system and the $p\pi_s^+$ system. For the (π_s^+p) system, in both regions, only moments with $I = 0,2$ are significantly different from zero, and therefore are compatible with a pure Δ^{++} resonance. For the $(\pi_f^+\pi^-\pi^0)$ system in the η^0 region, moments with $I > 0$ are negligible; this suggests that only S-waves are present, which is confirmed by the uniform angular distribution (see Section 4). In the ω^0-region, the system $(\pi_f^+\pi^-\pi^0)$ has moments values significantly different from zero for $I = 0,2$ which is indicative for the presence of a state of defined spin and parity (ω^0, $J^P = 1^-$ resonance).

3. HELICITY AMPLITUDE ANALYSIS

In this section, we use the helicity formalism to determine the amplitudes for the reaction $\pi^+p \to \Delta^{++}(\pi^+\pi^-\pi^0)$ in the η^0 and ω^0 regions. We must take in account the spin and helicity of the $(\pi^+\pi^-\pi^0)$ system and the helicity of the resonance Δ^{++}, decaying in proton and π^+. Using unpolarized targets, it is usually not possible to determine all the helicity amplitudes, because the number of independent observables is smaller than the number of amplitudes[6]. It is necessary to reduce the

number of independent amplitudes to be determined, by assuming hypotheses based on models. We assume that the relative spin between the target proton and the Δ^{++} is 1, corresponding to the class A relations derived from the additive quark model [3].

3.1 - ω^0 Region

The 24 helicity amplitudes corresponding to all possible orientations of the spin of the involved particles in the reaction, are reduced to 12 independent amplitudes by parity conservation. Assuming that the only possible value for the relative spin between the target proton and the Δ^{++} is 1, we reduce the number of independent complex amplitudes to 5, resulting in 9 real parameters to be determined (a common phase is arbitrary). The following 5 independent amplitudes $T^{\Lambda_\omega \eta}_{\Lambda_\Delta \lambda_b}$ are used in this analysis:

$$T^{0-}_{1/2\ 1/2}\ T^{0-}_{3/2\ 1/2}\ T^{1-}_{1/2\ 1/2}\ T^{1-}_{3/2\ 1/2}\ T^{1+}_{3/2\ 1/2}$$

where Λ_ω, Λ_Δ and λ_b correspond to the helicity of ω^0, Δ^{++} and target proton, respectively, and η denotes the exchange naturality. The amplitudes are determined for intervals of $t' = t - t_{min}$, the squared four-momentum transfer from p to Δ^{++}, by a maximum likelihood fit using the experimental data and the following expression for the differential cross section parametrized on these amplitudes (eq. A9.a of reference [4]):

$$\frac{d\sigma}{dt\,d\cos\theta\,d\phi\,d\cos\beta\,d\alpha} = \left(\frac{2\pi}{p_a}\right)^2 \times \frac{4\pi}{s} \times \frac{1}{2} \sum_{\lambda_b \lambda_p} \left| f_{\lambda_b \lambda_p} \right|^2$$

with

$$\frac{1}{\sqrt{2}} f_{\lambda_b \lambda_p} = \sum_{\Lambda_\Delta \Lambda_\omega} \sqrt{\frac{3}{8\pi^2}} D^{3/2*}_{\Lambda_\Delta \lambda_p}(\Phi\Theta) D^{1*}_{\Lambda_\omega,0}(\alpha\beta) T^{\Lambda_\omega}_{\Lambda_\Delta \lambda_b}(s,t) \quad ,$$

where s is the centre of mass (c.m.) energy of the reaction; p_a is the c.m. momentum of the π^+ beam; λ_p is the helicity of the outgoing proton; Φ,Θ are the azimuthal and polar angle of the proton in the Gottfried-Jackson (GJ) rest system of Δ^{++}; α, β are the azimuthal and polar angle describing the direction of the normal to the decay plane ($\omega^0 \to \pi^+\pi^-\pi^0$) in the GJ rest system of ω^0[7].

Introducing the amplitudes $T^{\Lambda_\omega \eta}_{\Lambda_\Delta \lambda_b}$ with definite exchange naturality η, where $\eta = +1$ (-1) corresponds to natural (unnatural) parity exchange, which is defined by

$$T^{\Lambda_\omega \eta}_{\Lambda_\Delta \lambda_b} = C_{\eta \Lambda_\omega} \left(T^{\Lambda_\omega}_{\Lambda_\Delta \lambda_b} + \eta (-1)^{\Lambda_\omega + 1} T^{-\Lambda_\omega}_{\Lambda_\Delta \lambda_b} \right)$$

with

$$C_{\eta \Lambda_\omega} = \begin{cases} \frac{1}{2} & \text{for } \Lambda_\omega = 0 \quad , \quad \eta = - \\ -i\frac{1}{2} & \text{for } \Lambda_\omega = 0 \quad , \quad \eta = + \\ \sqrt{2}/2 & \text{for } \Lambda_\omega \neq 0 \quad , \quad \eta = - \\ -i\frac{\sqrt{2}}{2} & \text{for } \Lambda_\omega \neq 0 \quad , \quad \eta = + \end{cases}$$

we have:

$$\frac{1}{\sqrt{2}} f_{\lambda_b \lambda_p} = \sum_{\substack{\Lambda_\omega \geq 0 \\ \eta}} E^{(\alpha,\beta)}_{\Lambda_\omega \eta} \sum_{\Lambda_\Delta} \frac{1}{\sqrt{2\pi}} D^{3/2*}_{\Lambda_\Delta \lambda_p}(\Phi,\Theta) T^{\Lambda_\omega \eta}_{\Lambda_\Delta \lambda_b}$$

where

$$E_{\Lambda_\omega \eta} = \sqrt{\frac{3}{4\pi}} C_{\eta \Lambda_\omega} \left[D^{1*}_{\Lambda_\omega 0}(\alpha,\beta) - \eta D^{1}_{\Lambda_\omega 0}(\alpha,\beta) \right]$$

Introducing the amplitudes $\tilde{T}^{\Lambda_\omega \eta}_{1H}$ defined on a basis with definite $p\Delta^{++}$ spin s = 1 and helicity H (according to [4]), we have

$$\frac{1}{\sqrt{2}} f_{\lambda_b \lambda_p} = \sum_{\substack{\Lambda_\omega \geq 0 \\ \eta}} E_{\Lambda_\omega \eta} \sum_H \frac{1}{\sqrt{2\pi}} D^{3/2*}_{H+\lambda_b, \lambda_p}(\Phi,\Theta) \frac{3}{4C_{\eta H}} < \frac{1}{2}, \lambda_b, 1, H \left| \frac{3}{2}, H+\lambda_b \right. > \tilde{T}^{\Lambda_\omega \eta}_{1H}$$

$$= \sum_{\substack{\Lambda_\omega \geq 0 \\ \eta H \geq 0}} \sqrt{3} \; E_{\Lambda_\omega \eta}(\alpha,\beta) \; \tilde{A}^{\lambda_b \lambda_p}_{H\eta}(\Phi\Theta) \; \tilde{T}^{\Lambda_\omega \eta}_{1H}$$

where $$\tilde{A}^{\lambda_b \lambda_p}_{0-}(\Phi\Theta) = \frac{1}{C_{-0}} \sqrt{\frac{3}{32\pi}} < \frac{1}{2}, \lambda_b, 1, 0 \left| \frac{3}{2}, \lambda_b \right. > D^{3/2*}_{\lambda_b \lambda_p}(\Phi,\Theta)$$

and

$$\tilde{A}^{\lambda_b \lambda_p}_{1\eta}(\Phi\Theta) = \frac{1}{C_{\eta 1}} \sqrt{\frac{3}{32\pi}} \{ < \frac{1}{2}, \lambda_b, 1, 1 \left| \frac{3}{2}, \lambda_b + 1 \right. > D^{3/2*}_{\lambda_b+1, \lambda_p}(\Phi,\Theta) +$$

$$+ \eta < \frac{1}{2}, \lambda_b, 1, -1 \left| \frac{3}{2}, \lambda_b - 1 \right. > D^{3/2*}_{\lambda_b - 1 \lambda_p}(\Phi,\Theta) \}$$

The normalization was done taking as factor the value of

$$\frac{d\sigma}{dt} = \int \frac{d\sigma}{dt d\cos\Theta d\Phi d\cos\beta d\alpha} \, d\cos\Theta d\Phi d\cos\beta d\alpha \quad .$$

3.2 - η^0 Region

Considering the parity conservation and assuming the value for the relative spin between the proton target and Δ^{++} to be 1, the 8 complex amplitudes which describe the reaction

$\pi^+p \to \Delta^{++}(\pi^+\pi^-\pi^0)$ in the η^0 region, are reduced to only 2 independent ones with a fixed overall phase, so that only 3 real parameters are to be determined.

The following 2 independent amplitudes $T^{\Lambda_{\eta^0}\eta}_{\Lambda_\Delta \lambda_p}$ are used in this analysis:

$$T^{0+}_{\frac{3}{2}\,\frac{1}{2}} \qquad \text{and} \qquad T^{0+}_{\frac{1}{2}\,\frac{1}{2}}$$

These amplitudes are determined in intervals of t', by the same procedure as used in the ω^0 region, taking in account that η^0 is a resonance with $J^P = 0^-$.

4. RESULTS

The absolute phases of the amplitudes can not be determined. We choose as reference, the phase of the amplitude $T^{0-}_{3/2\ 1/2}$ (for the ω^0 region) and $T^{0+}_{3/2\ 1/2}$ (for the η^0 region) imposing for these amplitudes the phase zero, that is, the value of these amplitudes become real and positive.

In Fig. 6 and Fig. 9 we show, for the ω^0 and η^0 region, respectively, the t' dependence of the amplitudes for the reaction $\pi^+p \to \Delta^{++}(\pi^+\pi^-\pi^0)$ as a result of the above mentioned fit.

Fig. 7 and Fig. 10 show the behaviour of the relative phases of the correspondent amplitudes.

To check the results we show in Fig. 8 and Fig. 11 a comparison between the experimental angular distributions (full lines) in GJ system and those created from the amplitudes (dotted lines).

It is seen that the agreement is very good, that is, the s = 1 constraint is applicable to our problem.

5. CONCLUSIONS

5.1 - ω^0 Region

Since the ω^0 production in the reaction $\pi^+p \to \Delta^{++}\omega^0$ can proceed only via the exchange of a particle of G parity +1, isospin 1 or 2 and $J^P = 0^+$ is not allowed, the known candidates for the exchanged particles, corresponding to the cross section σ^{1+} for the natural parity exchange, is the ρ meson, whereas that corresponding to the cross section σ^- for the unnatural parity exchange is the B meson.

According to the s-dependence of the amplitudes in the Regge-Pole theory, we may write

$$R_{f\ \Lambda_\Delta \Lambda_b}^{\Lambda_\omega} \propto \left(\frac{s}{s_0}\right)^{\alpha^R(t)}$$

where R denotes the type of the exchange, $s_0 = 1\ GeV^2$, and $\alpha_R(t)$ is the Regge trajectory parametrized as $\alpha^R(t) = \alpha_0^R + \alpha'^R t$. Using $\alpha^\rho(t) = 0.55+0.9t$ as the ρ Regge trajectory, we can compare our results of the cross section σ^{1+} at 16 GeV/c with those at 7,1 GeV/c[1].

Fig. 12 shows this comparison. Full circles represent data at 7.1 GeV/c and open circles give our results at 16 GeV/c. The dashed line is the extrapolation at 7.1 GeV/c of our results obtained at 16 GeV/c using the above mentioned Regge model s-dependence of the amplitude and the ρ trajectory. We can conclude that

the assumption of ρ exchange for the cross section σ^{1+} is compatible with the energy dependence found for this component.

As can be seen in Fig. 12, the t' behaviour of σ^{1+} shows no evidence for a dip near $t' \approx 0{,}6\ GeV^2$, which is the position of the nonsense wrong-signature-zero of the ρ particle. Such a dip was also not found by other authors[1].

Comparing the results obtained for the amplitudes, we note that the amplitude $T^{1+}_{3/2\ 1/2}$, which is the only amplitude for natural parity exchange, is dominant in the whole interval of t'; this indicates that the mechanism of ρ exchange is the principal mechanism but not the only one.

Fig. 13 shows the differential cross section dσ/dt due to unnatural parity exchange as function of t'. By comparing Fig. 13 and Fig. 12, it can be seen that not only the natural but also the unnatural parity exchange contributes over the whole range of t' studied. A dip near $t' = 0{,}2\ GeV^2$ is seen in the behaviour of the cross section σ^-, which may be explained by the nonsense wrong-signature-zero of the B meson exchange.

Integrating over the momentum transfer and taking for the cross section of the reaction $\pi^+p \to \Delta^{++}\omega^0$ the value $(27 \pm 3)\mu b$[8], we obtain for the cross-sections, due to the natural and unnatural parity exchange, the values $15.2 \pm 2.7\mu b$ and $11.8 \pm 1.7\ \mu b$, respectively.

Analysing the t' dependence of the different amplitudes (Fig. 9) we conclude that in producing the reaction $\pi^+p \to \Delta^{++}\omega^0$, the contribution with unnatural parity exchange is predominantly due to the amplitude $T^{0-}_{1/2\ 1/2}$, that is, when there is no flip of the barion helicity and ω^0 has zero helicity.

5.2 - η^0 Region

The η^0 production in the reaction $\pi^+ p \to \Delta^{++}\eta^0$ can proceed only via the exchange of a particle of G parity -1, isospin 1 and $J^P = 0^+, 1^-, 2^+ \ldots$ The most probable candidate for the exchanged particle is the A_2 meson. As we can see in Fig. 9, both amplitudes contribute to the production of η^0 in this reaction, in whole t' interval studied, whith a dominance, at small t' values , of the barion flip helicity on the $pA_2\Delta^{++}$ vertex. This fact is in agreement with the assumption made in the dual absorption model for dips in inelastic hadron processes[9], which predicts no dip for the reaction $\pi N \to \eta\Delta$. In our results we found no evidence for such dips (Fig. 9).

FIGURE CAPTION

FIG. 1 - Mass distribution of the $p\pi_s^+$ system. For the middle histogram, the ω^0 resonance region ($0{,}72 \leq M(\pi_f^+\pi^-\pi^0) \leq 0.81$ GeV) is selected. For the upper histogram the η^0 resonance region ($0.52 \leq M(\pi_f^+\pi^-\pi^0) \leq 0.60$ GeV) is selected.

FIG. 2 - Mass distribution of the $\pi_f^+\pi^-\pi^0$ system. For the shaded histogram, the Δ^{++} resonance region ($1.08 \leq M(p\pi_s^+) \leq 1.4$ GeV) is selected. The two upper histograms are restricted to the regions of the η^0 and ω^0 masses.

FIG. 3 - Mass distribution of the $p\pi_f^+$ system restricted to the conditions: $0{,}72 \leq M(\pi_f^+\pi^-\pi^0) \leq 0.81$ GeV and $1.08 \leq M(p\pi_s^+) \leq 1.4$ GeV.

FIG. 4 - Normalized moments $\langle D^J_{M0} \rangle$ of the $\pi^+\pi^-\pi^0$ and $p\pi^+$ systems for the η^0 region.

FIG. 5 - Normalized moments $\langle D^J_{M0} \rangle$ of the $\pi^+\pi^-\pi^0$ and $p\pi^+$ systems for the ω^0 region.

FIG. 6 - Amplitudes $T^{\Lambda_\omega \eta}_{\Lambda_\Delta \lambda_p}$ as functions of t' for the reaction $\pi^+p \to \Delta^{++}\omega^0$.

FIG. 7 - Phases $\phi^{\Lambda_\omega \eta}_{\Lambda_\Delta \lambda_p}$ relative to the amplitude $T^{0-}_{3/2\ 1/2}$ as functions of t' for the reaction $\pi^+p \to \Delta^{++}\omega^0$.

FIG. 8 - Experimental angular distributions of Δ^{++} and ω^0 (full lines) in the G.J. system together with the created angular distributions (dotted lines) using the amplitudes of the reaction $\pi^+p \to \Delta^{++}\omega^0$.

FIG. 9 - Amplitudes $T^{\Lambda_\omega \eta}_{\Lambda_\Delta \lambda_p}$ as functions of t' for the reaction $\pi^+p \to \Delta^{++}\eta^0$.

FIG. 10 - Phases $\phi^{\Lambda_{\eta^0\eta}}_{\Lambda_\Delta \lambda_p}$ relative to the amplitude $T^{0+}_{3/2\ 1/2}$ as functions of t' for the reaction $\pi^+p \to \Delta^{++}\eta^0$.

FIG. 11 - Experimental $\cos\theta$ distribution of Δ^{++} and η^0 (full lines) in the helicity system together with the created angular distributions (dotted lines) using the amplitudes of the reaction $\pi^+p \to \Delta^{++}\eta^0$.

FIG. 12 - Comparison between the natural parity exchange cross sections for the reaction $\pi^+p \to \Delta^{++}\omega^0$ at 16 GeV/c (open circles) and at 7.1 GeV/c (closed circles) (ref. [1]) as function of t'. The curve is described in the text.

FIG. 13 - Unnatural parity exchange cross section for the reaction $\pi^+p \to \Delta^{++}\omega^0$ at 16 GeV/c as function of t'.

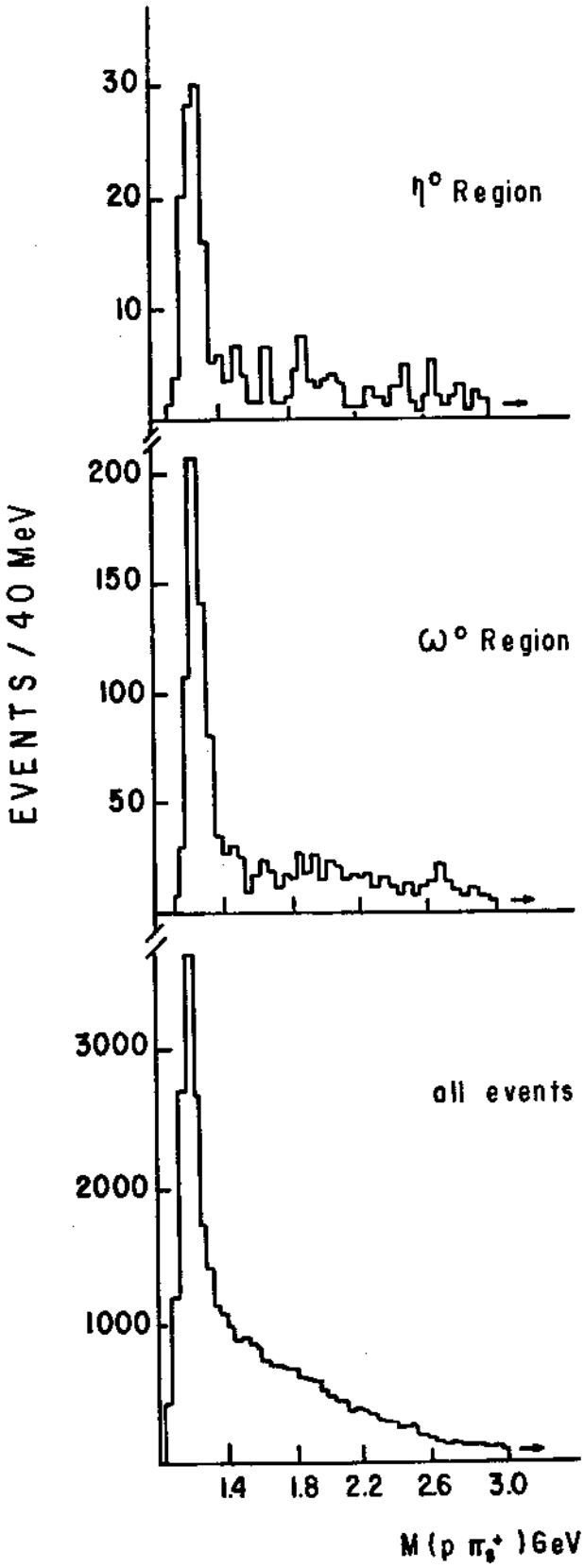
30
20
10
η° Region
200
150
100
50
ω° Region
3000
2000
1000
all events
EVENTS / 40 MeV
1.4
1.8
2.2
2.6
3.0
M (p π₀⁺) GeV

FIG.1

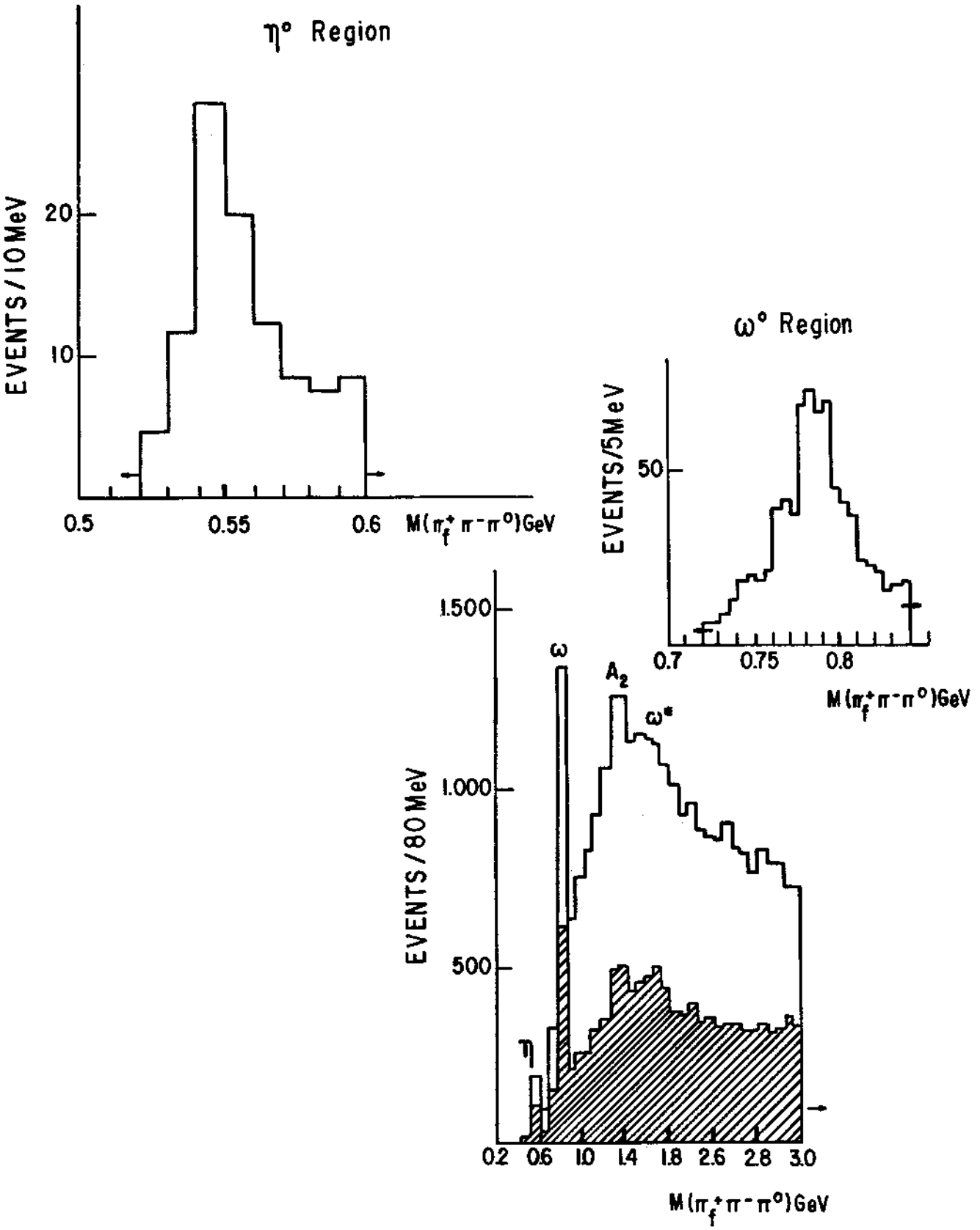
η° Region
EVENTS/10MeV
20
10
0.5
0.55
0.6
M(π⁺f π⁻π°)GeV
ω° Region
EVENTS/5MeV
50
0.7
0.75
0.8
M(π⁺f π⁻π°)GeV
EVENTS/80MeV
1.500
1.000
500
ω
A2
ω*
η
0.2
0.6
1.0
1.4
1.8
2.6
2.8
3.0
M(π⁺f π⁻π°)GeV

FIG.2

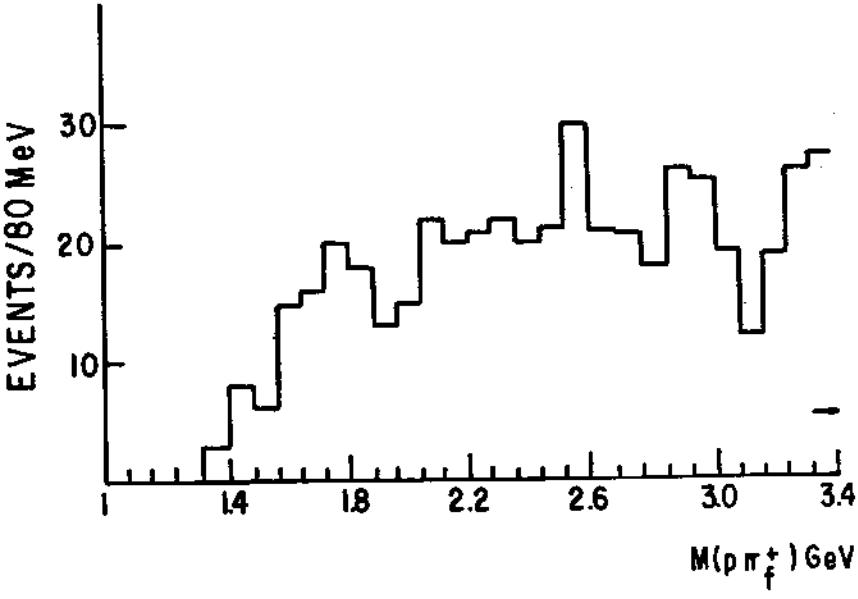

FIG. 3

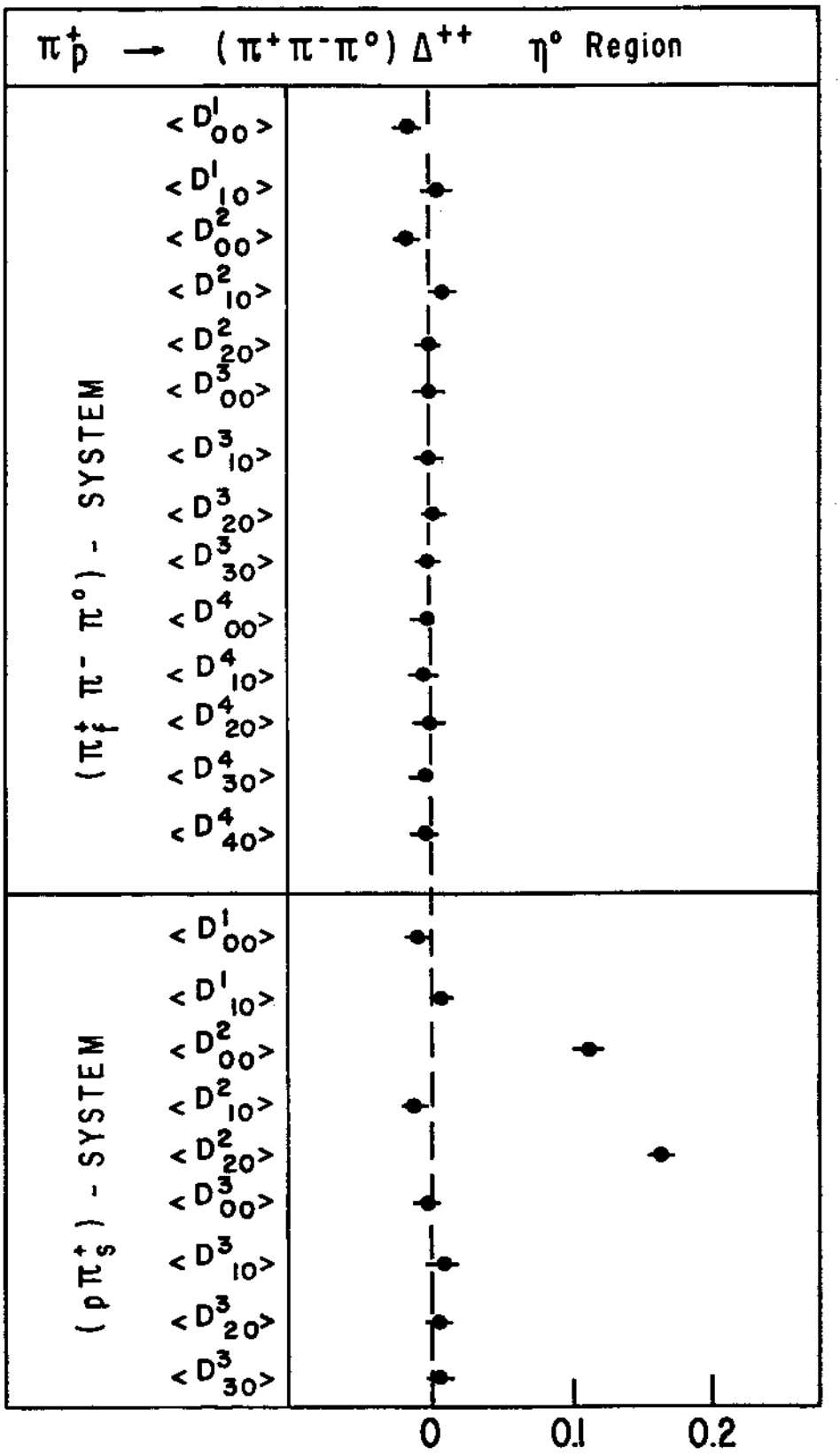
$\pi^+ p \rightarrow (\pi^+\pi^-\pi^0)\,\Delta^{++}$ η^0 Region
$(\pi_f^+\,\pi^-\,\pi^0)$ - SYSTEM
$(p\,\pi_s^+)$ - SYSTEM
$\langle D^1_{00}\rangle$
$\langle D^1_{10}\rangle$
$\langle D^2_{00}\rangle$
$\langle D^2_{10}\rangle$
$\langle D^2_{20}\rangle$
$\langle D^3_{00}\rangle$
$\langle D^3_{10}\rangle$
$\langle D^3_{20}\rangle$
$\langle D^3_{30}\rangle$
$\langle D^4_{00}\rangle$
$\langle D^4_{10}\rangle$
$\langle D^4_{20}\rangle$
$\langle D^4_{30}\rangle$
$\langle D^4_{40}\rangle$
0
0.1
0.2

FIG. 4

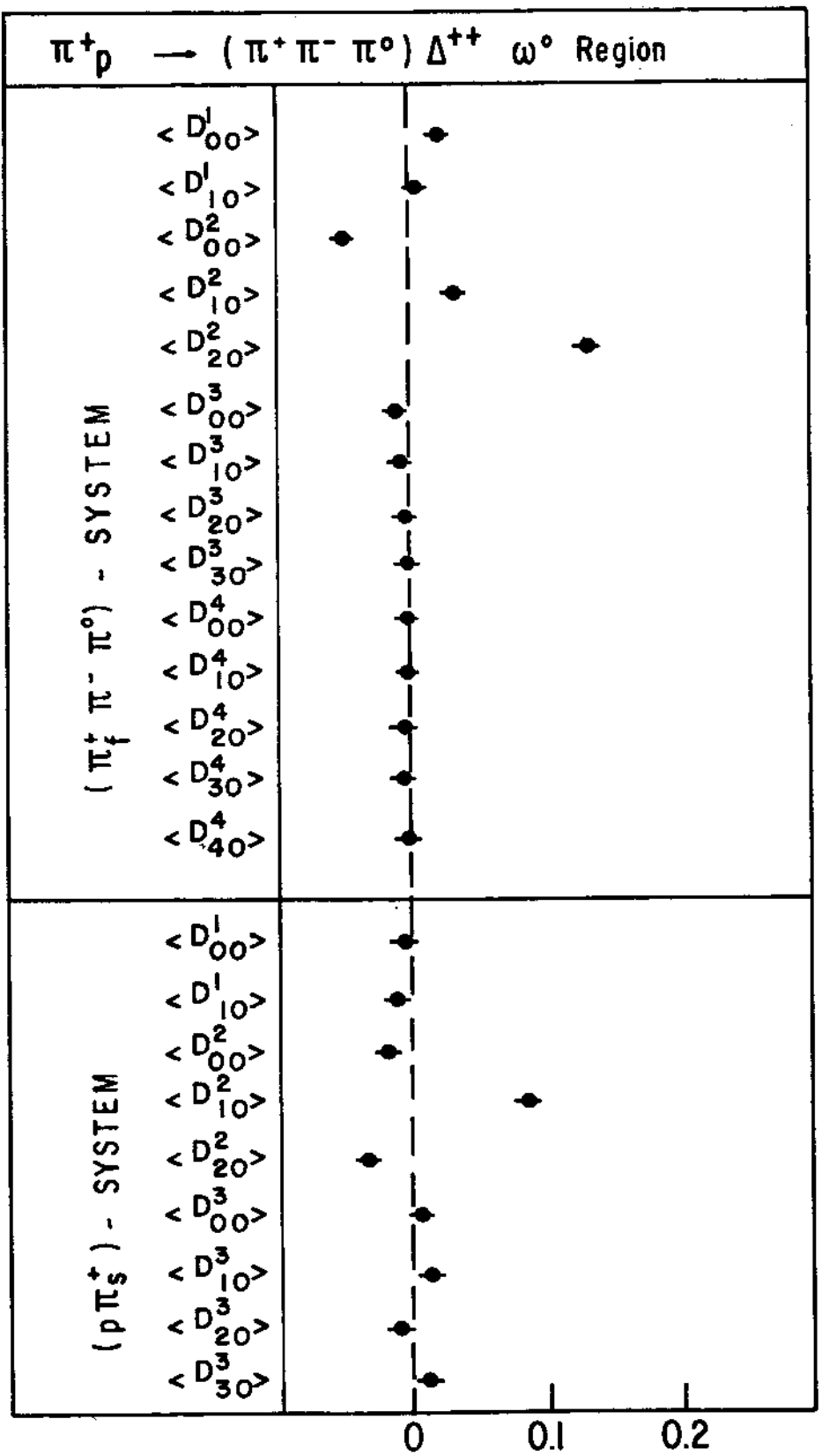
$\pi^+ p \longrightarrow (\pi^+ \pi^- \pi^0)\, \Delta^{++}$ ω^0 Region
$(\pi_f^+ \pi^- \pi^0)$ - SYSTEM
$(p \pi_s^+)$ - SYSTEM
$\langle D^1_{00} \rangle$
$\langle D^1_{10} \rangle$
$\langle D^2_{00} \rangle$
$\langle D^2_{10} \rangle$
$\langle D^2_{20} \rangle$
$\langle D^3_{00} \rangle$
$\langle D^3_{10} \rangle$
$\langle D^3_{20} \rangle$
$\langle D^3_{30} \rangle$
$\langle D^4_{00} \rangle$
$\langle D^4_{10} \rangle$
$\langle D^4_{20} \rangle$
$\langle D^4_{30} \rangle$
$\langle D^4_{40} \rangle$
0
0.1
0.2

FIG. 5

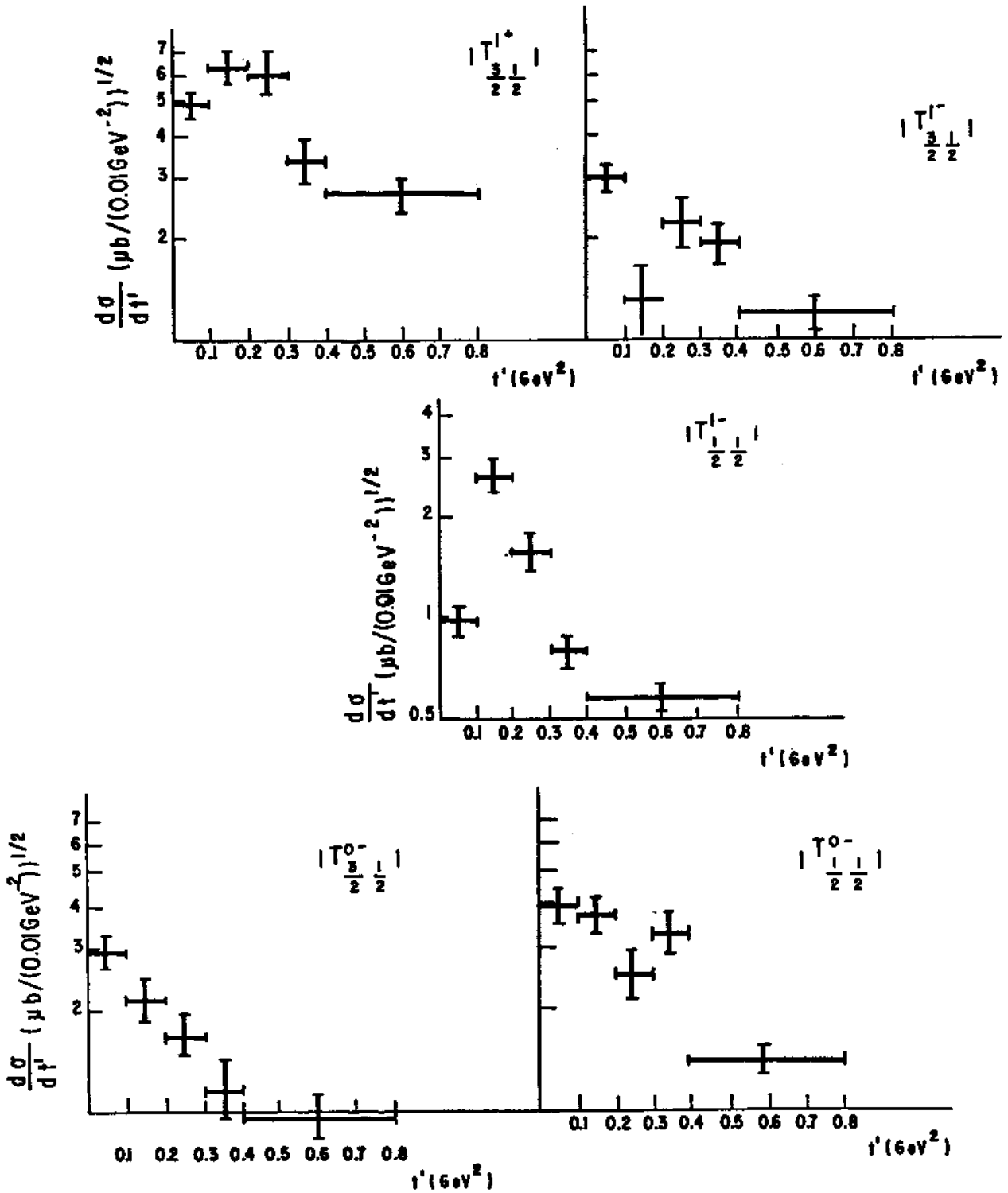
$\frac{d\sigma}{dt'}$ (μb/(0.01GeV^{-2}))$^{1/2}$
$|T^{1+}_{\frac{3}{2}\frac{1}{2}}|$
$|T^{1-}_{\frac{3}{2}\frac{1}{2}}|$
$|T^{1-}_{\frac{1}{2}\frac{1}{2}}|$
$|T^{0-}_{\frac{3}{2}\frac{1}{2}}|$
$|T^{0-}_{\frac{1}{2}\frac{1}{2}}|$
t'(GeV^2)

FIG. 6

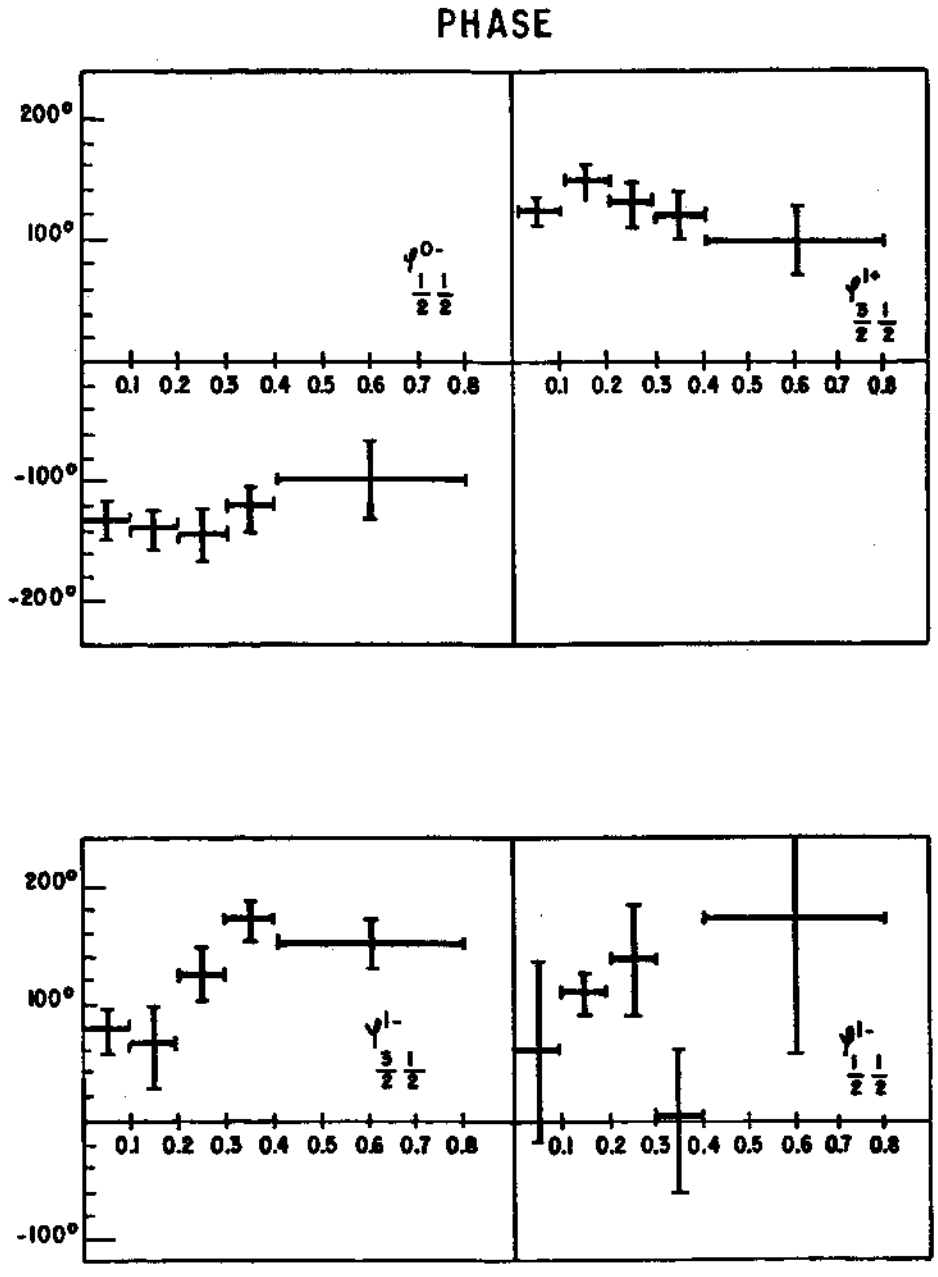
PHASE
200°
100°
-100°
-200°
$\psi^{0-}_{\frac{1}{2}\frac{1}{2}}$
$\psi^{1+}_{\frac{3}{2}\frac{1}{2}}$
$\psi^{1-}_{\frac{3}{2}\frac{1}{2}}$
$\psi^{1-}_{\frac{1}{2}\frac{1}{2}}$
0.1 0.2 0.3 0.4 0.5 0.6 0.7 0.8

FIG.7

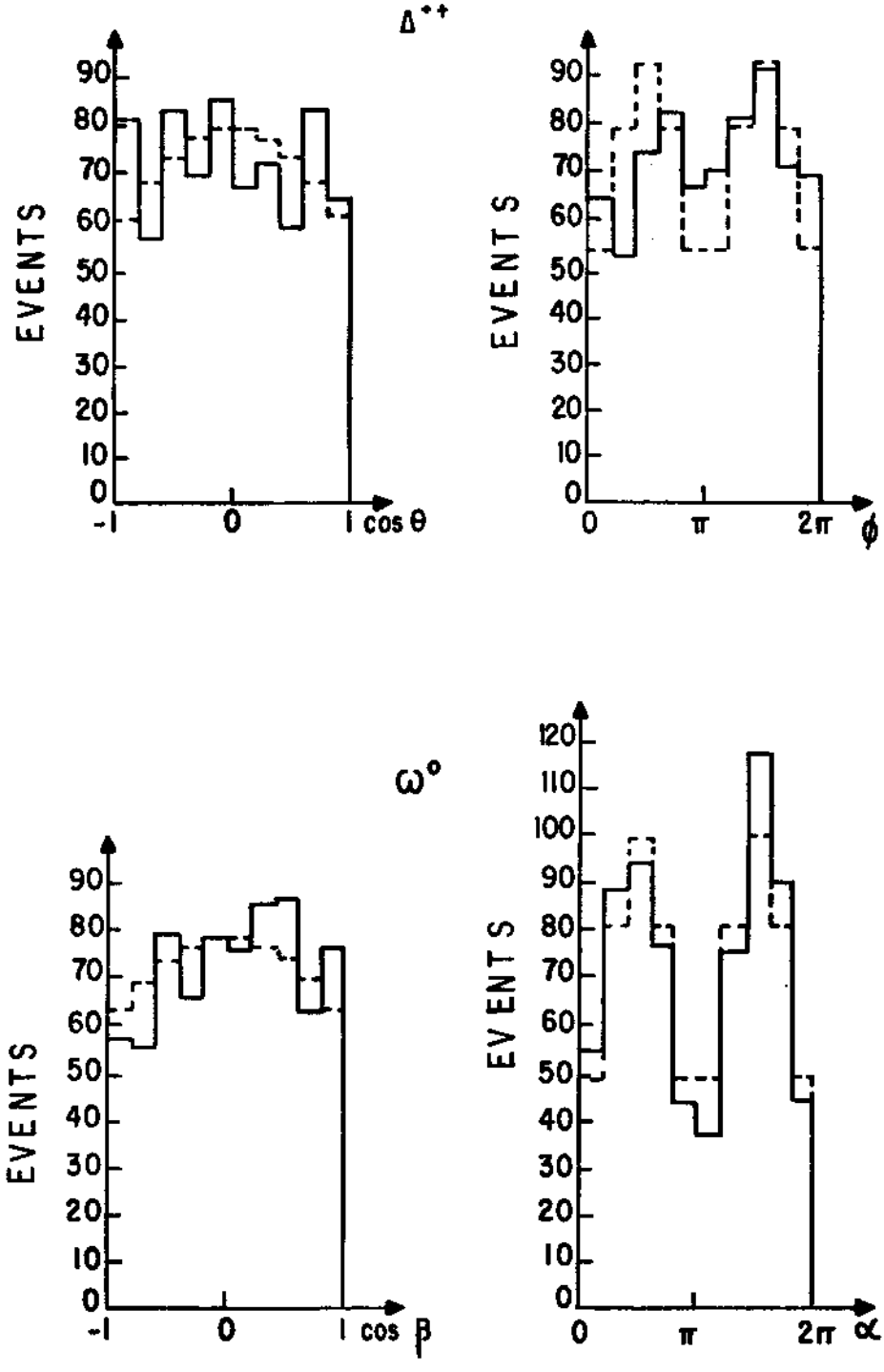

ANGULAR DISTRIBUTION

G J SYSTEM

FIG.8

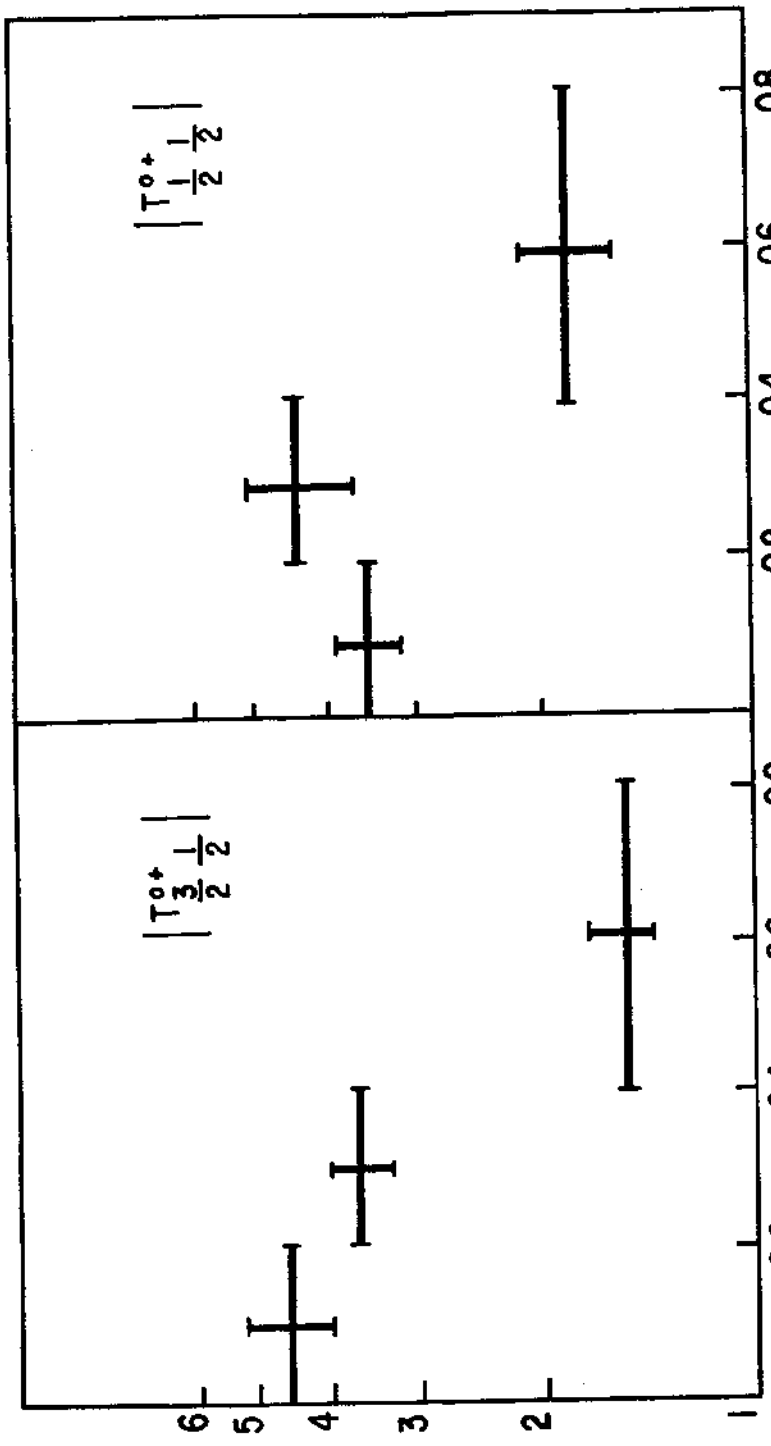
$\left|T^{0+}_{\frac{3}{2}\frac{1}{2}}\right|$
$\left|T^{0+}_{\frac{1}{2}\frac{1}{2}}\right|$
$\frac{d\sigma}{dt'}$ (μb/(0.01 GeV^{-2}))$^{1/2}$
t'(GeV^2)
t'(GeV^2)

FIG. 9

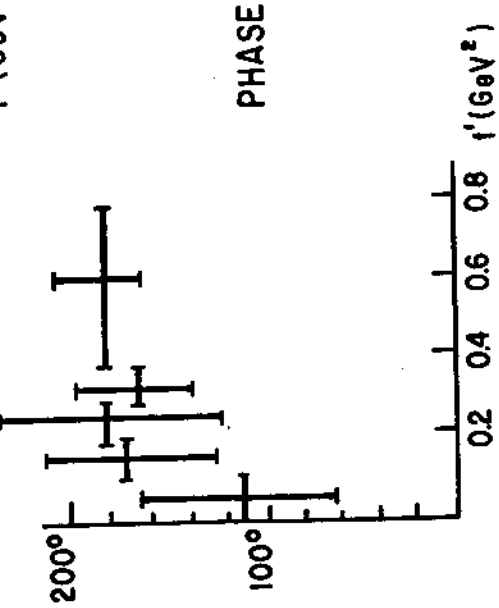
PHASE
200°
100°
t'(GeV^2)

FIG. 10

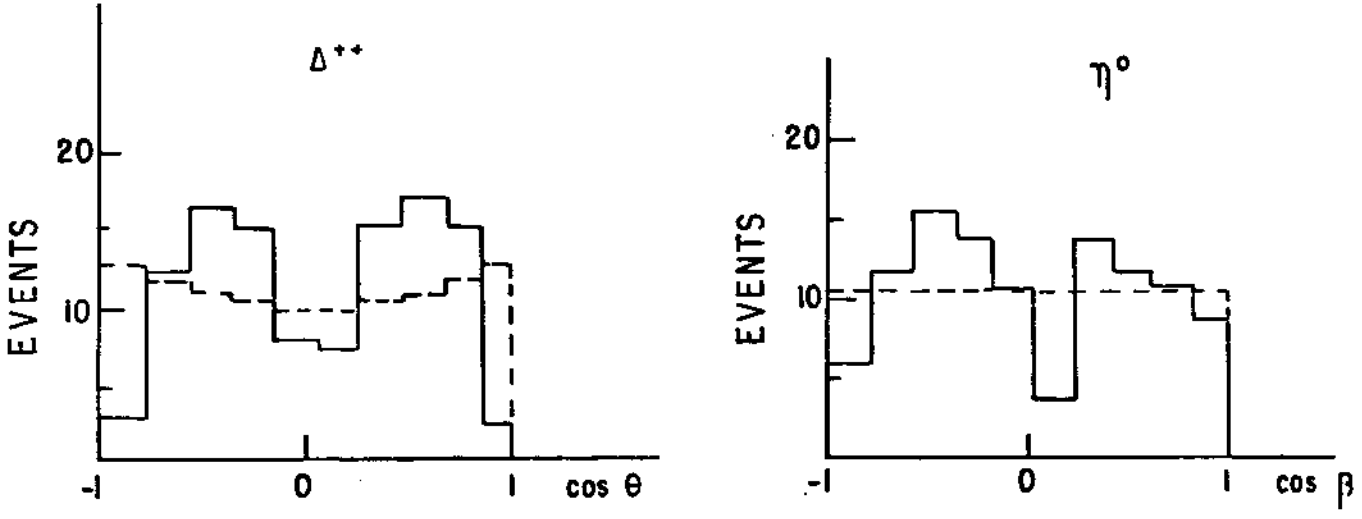

FIG. 11

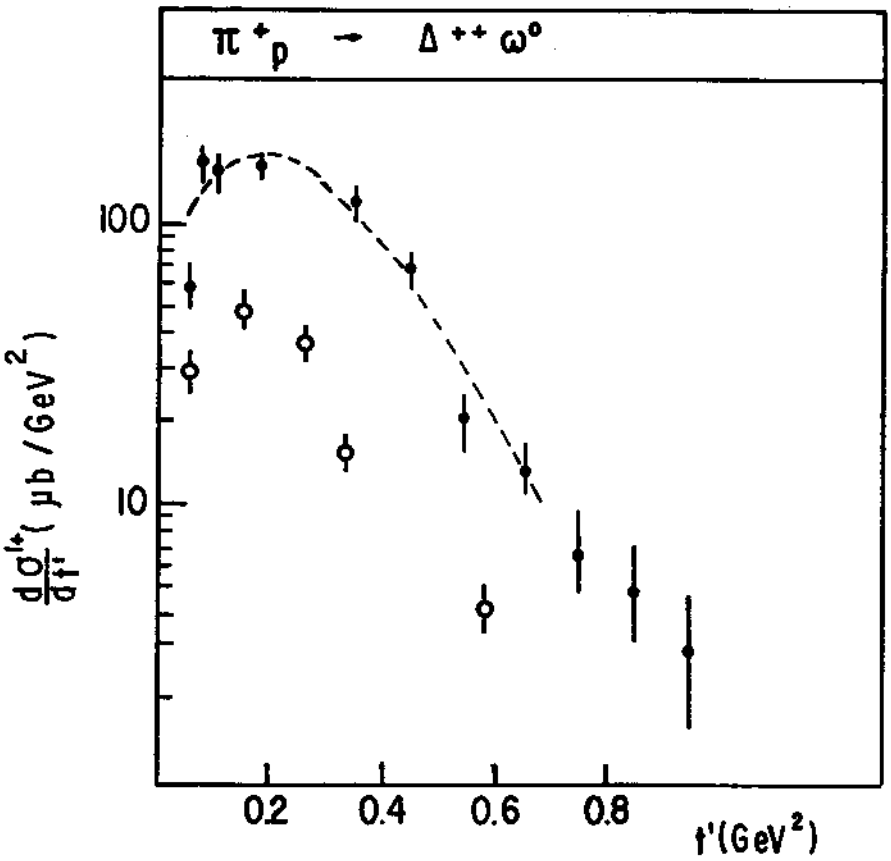
π⁺p → Δ⁺⁺ω°
100
10
dσ⁺⁺/dt' (μb/GeV²)
0.2
0.4
0.6
0.8
t'(GeV²)

FIG. 12

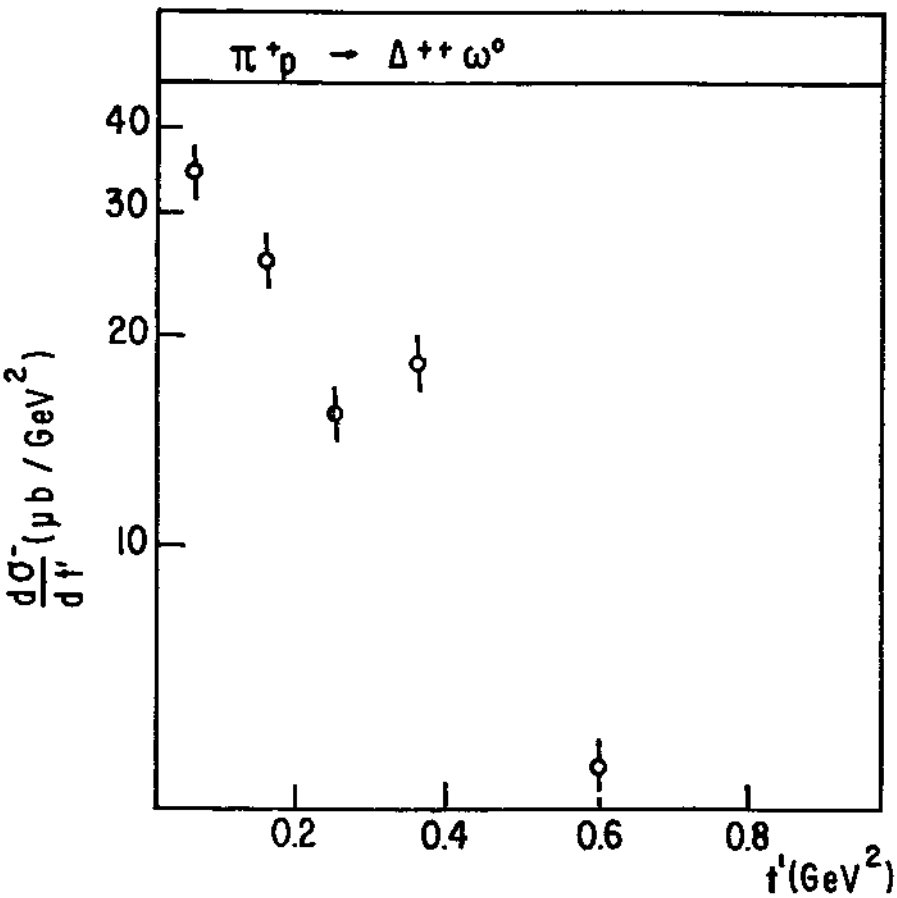
π⁺p → Δ⁺⁺ω°
40
30
20
10
dσ⁻/dt' (μb/GeV²)
0.2
0.4
0.6
0.8
t'(GeV²)

FIG. 13

REFERENCES

[1] J.F. Owens et al, Nuclear Physics B94(1975) 77-99; Phys. Letters 58B(1975)376; Nuclear Physics B112(1976)514).

[2] W. Schmitz, Thesis RWTH Aachen 1978 (unpublished).

[3] A. Białas and K. Zalewski, Nuclear Physics B6(1968) 449, 465,478.

[4] H. Laven et al., Nuclear Physics B137(1978)202.

[5] H. Laven, Thesis RWTH Aachen - 1977.

[6] M.G. Doncel et al., Fortschritte der Physik 24(1976)259.

[7] S.U. Chung, Spin Formalisms - CERN - 71-8(1971).

[8] H. Grässler et al., Nuclear Physics B115(1976)365.

[9] H. Harari, Phys. Rev. Letters 26(1971)1400.